This article has been accepted for publication in a future issue of this journal, but has not been fully edited. Content may change prior to final publication. Citation information: DOI 10.1109/LPT.2018.2863559, IEEE Photonics Technology Letters

Off-peak dual-wavelength multimode diode-laser-pumped fiber Raman laser

Soonki Hong, Yutong Feng, and Johan Nilsson

***Abstract*—We demonstrate a fiber Raman laser directly pumped by two spectrally combined multimode diode lasers at ~950 nm and ~976 nm. The emission wavelength becomes 1020 nm, which corresponds to the 1st Stokes of 976 nm. The pump separation of 270 cm^{-1} is both much smaller than the Raman peak shift of 440 cm^{-1} and much larger than the Raman linewidth of around 100 cm^{-1}, which is unfavorable for efficient Raman conversion. Nevertheless, the addition of the pump at 950 nm triples the output power compared to pumping only at 976 nm. We reach 23 W of output power with slope efficiency of 51% and beam quality M^2 of 5.2 in a germanosilicate graded-index fiber.**

***Index Terms*— Fiber lasers, Fiber nonlinear optics, Raman Lasers.**

I. Introduction

Fiber Raman lasers (FRLs) [1], [2] are attractive for their wavelength versatility and compatibility with well-established, well-controlled, fiber fabrication processes, e.g., of germanosilicate fibers for telecom transmission. However, the underlying stimulated Raman scattering (SRS) is a weak nonlinearity [1], and therefore, it is necessary to pump with high pump intensities. Although kW-level FRLs are still possible with high-brightness pump sources such as Yb-doped fiber lasers [3], the attraction of this approach is impaired by the overall system efficiency and complexity, the limited enhancement or even degradation of the brightness, and the limited availability of practical pump wavelengths. Alternatively, pumping directly with diode lasers offers additional pump wavelengths in a simpler system, and potentially higher efficiency. However, the brightness of conventional high-power multimode diode lasers is still marginal, so SRS requires long fibers in which propagation loss reduces the efficiency. Furthermore, the potential for enhancing the spatial brightness is lower in cladding-pumped FRLs than in their rare-earth-doped counterparts [4]. Thus, though directly diode-pumped FRLs have been power-scaled to 154 W with 65% optical-to-optical efficiency and three times brightness enhancement using graded-index (GRIN) fiber [5] and reached 9.6 times brightness enhancement in a double-clad fiber [6], further progress in power and brightness rely on improved diode lasers for pumping.

At the same time, there is a strong development of high-power multi-wavelength diode laser sources for materials processing [7], [8]. Whereas these reach brightnesses considerably higher than the 0.17 W sr^{-1} μm^{-2} we used in our previous diode-pumped FRL work [6], their total spectral linewidth is typically significantly larger than the Raman gain bandwidth of around 100 cm^{-1} (~ 10 nm at 1 μm) in germanosilicate. Often it even exceeds the germanosilicate Raman shift of 440 cm^{-1}. This is a challenge when the objective is to generate Raman laser emission at a single wavelength. Although this is still possible [9], it becomes more difficult and may also reduce the efficiency, especially when the spectral separation of the pumps differs from the Raman peak shift.

In this paper, we demonstrate a FRL based on a multimode germanosilicate GRIN fiber pumped by two wavelength-combined multimode diode lasers at 950 nm and 976 nm. The experimental results were previously reported at CLEO [10], but we here present additional data and analysis. In contrast to previous works on wavelength-combined multimode diode laser pumping with pump separation much smaller than the Raman linewidth [6] or with pump separation similar to the Raman shift [9], the separation (270 cm^{-1}) is now both substantially larger than the Raman linewidth and substantially smaller than the shift to the Raman peak (440 cm^{-1}). We expect this separation to be close to the most challenging for any value smaller than 440 cm^{-1}. Nevertheless, with dual-wavelength pumping we reach 23 W of output power at 1020 nm (1st Stokes of 976 nm), compared to 7.8 W with 976-nm single-diode pumping. This shows that it is possible to transfer the power efficiently from two pump sources with such adverse wavelength spacing into a single Stokes line. We believe this opens up for FRLs pumped by high-power multi-wavelength diode lasers currently being developed for materials processing [7], [8].

II. Experimental Setup

Figure 1 shows our experimental setup. A wavelength-locked diode laser at 976 nm (nLight element e18) is spectrally combined in a dichroic mirror with another diode laser at ~ 950 nm (JDSU Stingray). Both diodes are pigtailed with 105/125 μm, 0.22 NA fiber and can deliver up to 140 W of power each, with 95% of the power within an NA of 0.15, according to specifications. The beams are collimated separately with f = 20 mm aspheric lenses and then combined in dichroic mirror DM1 (Layertec). The combined power reaches up to 235 W. The beam is then passed through an aperture of 4.5 mm diameter. This reduces the size of the combined beam, which improves

Manuscript received June 4, 2018; revised ? ?, ????; accepted ? ?, ????. Date of publication ? ?, ????; date of current version ? ?, ????. This work was supported by the Air Force Office of Scientific Research under grant FA9550-15-1-0041.

S. Hong, Y. Feng, J. Nilsson are with the Optoelectronics Research Centre, University of Southampton, Southampton SO17 1BJ, UK. (e-mail: s.hong@soton.ac.uk).

All data supporting this paper are openly available from the University of Southampton repository at https://doi.org/10.5258/SOTON/D0549.

Color versions of one or more of the figures in this letter are available online at http://ieeexplore.ieee.org.

Digital Object Identifier will be added here.

This article has been accepted for publication in a future issue of this journal, but has not been fully edited. Content may change prior to final publication. Citation information: DOI 10.1109/LPT.2018.2863559, IEEE Photonics Technology Letters

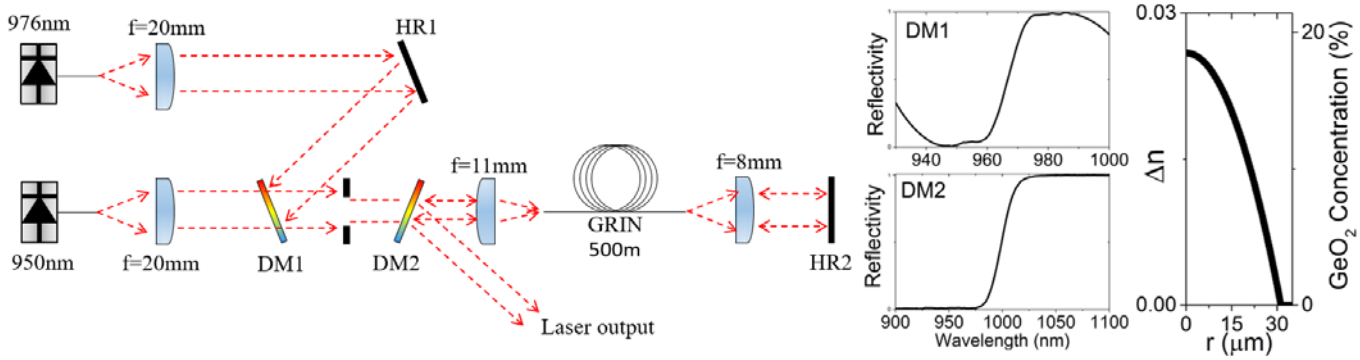

Fig. 1. Experimental setup. Inset graphs depict the reflectivity of DM1 and DM2 as well as the refractive index and GeO_2 concentration profile of GRIN fiber.

its beam quality. The power then drops to 176 W, i.e., to 74%. The aperture reduces the amount of pump light which is not coupled into the Raman gain fiber and thus instead adds to the thermal load at the fiber launch, which can lead to failure.

The combined pump beam passes through another dichroic mirror (DM2) with 98% transmission for the pump beam and > 97% reflection for the Stokes beam at 1020 nm and is then launched into the Raman gain fiber through an f = 11 mm aspheric lens (Thorlabs, C220TM-B).

The GRIN Raman gain fiber (OFS OM-4) is 500 m long and has a 62.5-μm diameter, 0.275-NA parabolic-index core and a 125-μm diameter cladding. This fiber is shorter than we used before [6], in order to avoid the build-up of higher Stokes orders even in the absence of any spectral filtering in the cavity. It is perpendicularly cleaved in both ends. The maximum incident pump power was measured before the focusing lens to 103 W for the 976-nm pump and to 72.5 W for the 950-nm pump. The launched maximum power was 49 W (976 nm) and 41 W (950 nm) with launch efficiency of 48% and 57%, respectively. We determined this by measuring the power transmitted through the fiber and compensating for the background loss of the fiber. In turn, we measured this to 3.44 dB/km (950 nm), 3.3 dB/km (975 nm), and 3.0 dB/km (1020 nm) by filling the core with white light and measuring the transmission through the 500-m length. The fiber was then cut back to a short length whereby the transmission loss was evaluated. These losses are almost twice of those of a longer fiber (1.5 km) of the same kind [6]. The difference may at least in part arise from mode-dependent loss, which can cause the attenuation to deviate from Beer-Lambert's law and lead to lower loss per unit length in longer fibers.

In the far end of the fiber, a collimating lens and a mirror (HR2) provided high-reflectivity feedback for the laser cavity. The mirror also reflected the pump back into the fiber in order to double-pass the pump. In the pump launch end, the perpendicular facet completed the cavity and served as a 4%-reflecting output coupler. After being reflected in DM2, the outcoupled beam was characterized with a thermal power meter and an optical spectrum analyzer. The power in different spectral bands was obtained by numerical integration of the optical spectra.

III. Results

We evaluated the FRL by gradually increasing the power of one pump while the other pump was either off or at full power. To evaluate the launched pump power, we blocked the feedback from the HR mirror and launched one pump at a time. This suppressed SRS, which would otherwise affect the transmitted pump power and thus the determination of the launch.

First, we varied the 976-nm pump power while the 950-nm pump was switched off. The curves (i) in Fig. 2 and in Fig. 3(a) show the results. The FRL emits at a wavelength of ~1020 nm. The threshold is approximately 15 W. The slope efficiency increases for higher pump power and reaches 36% for 30 W - 50 W of launched pump power.

The heatsinking of the 976-nm diode laser was inadequate for ensuring wavelength-locking over the full range of pump power, so the spectrum moves to longer wavelengths as the pump power increases. Fig. 3(a) shows spectra measured at the output of the fiber laser (following reflection in DM2). The unlocked part of the pump spectrum shifts from 973 nm at the threshold of the FRL to 983 nm at maximum power. At the same time, the output wavelength of the FRL increases from 1017 nm to 1024 nm.

Next, we varied the 950-nm pump power while the 976-nm diode was switched off. In this case, the peak Raman gain occurs around 990 nm, where the reflection of DM2 is small. Thus, the output power measured after DM2 is negligible when the FRL is pumped only by the 950-nm pump.

We then set the 950-nm pump to maximum power (41 W launched) and gradually increased the 976-nm pump. The

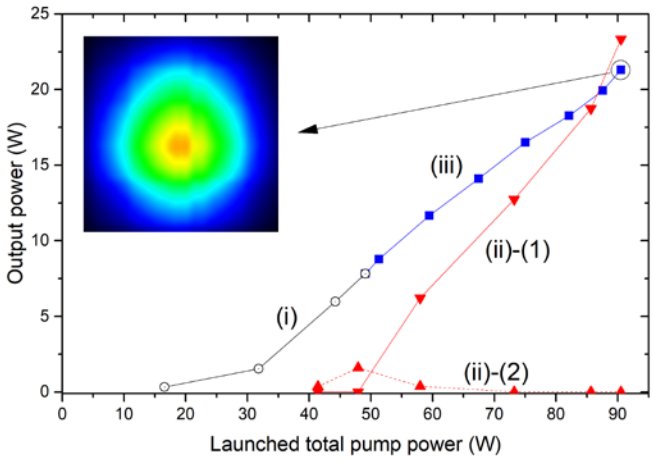

Fig. 2. FRL output power *vs.* launched total pump power. The labels on the curves indicate results for when (i) the 976-nm pump varies while the 950-nm pump is switched off, (ii) the 976-nm pump varies while the 950-nm pump is at maximum power (41 W), and (iii) the 950-nm pump varies while the 976-nm pump is at maximum power (49 W). Specifically, (ii)-(1) indicates the power of the primary signal at 1020 nm whereas (ii)-(2) indicates the power at 1000 nm (1st Stokes of the 950-nm pump), which is affected by a low reflectivity in DM2. The inset shows a 2D power distribution of maximum output power as created from orthogonal line scans.

This article has been accepted for publication in a future issue of this journal, but has not been fully edited. Content may change prior to final publication. Citation information: DOI 10.1109/LPT.2018.2863559, IEEE Photonics Technology Letters

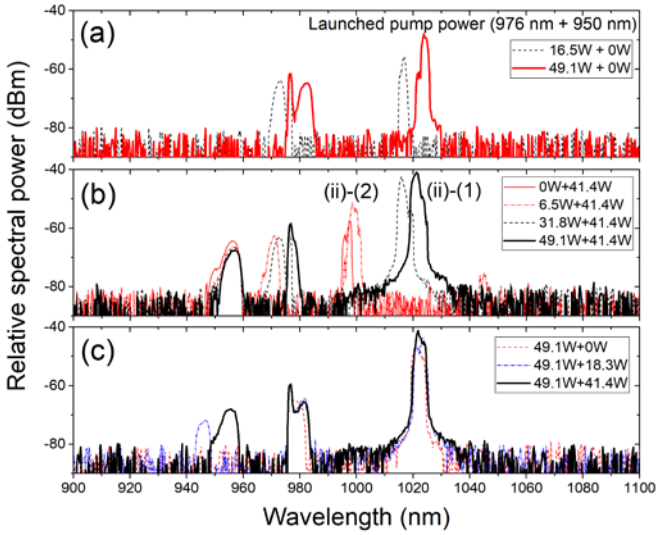

Fig. 3. Output spectra when (a) the 950-nm pump is switched off, (b) the 950-nm pump is at maximum power (41 W), (c) the 976-nm pump is at maximum power (49 W). In (b), (ii)-(1) indicates the primary signal (1020 nm) whereas (ii)-(2) (at 1000 nm) indicates 1st Stokes of the 950-nm pump.

curves (ii)-(1) and (ii)-(2) in Fig. 2 show the resulting output power, whereas Fig. 3(b) shows spectra at different pump levels. At low 976-nm pump powers (including when the 976-nm power is off), we see Raman Stokes emission at 990 – 1000 nm, although the low reflectivity of DM2 means that the power is low. There is also a small amount of second-order Stokes emission at 1045 nm.

When the launched 976-nm power exceeds 6.5 W (48 W of total launched pump power), FRL emission appears at ~1020 nm, i.e., at the 1st Stokes of 976 nm. The 1020-nm power then grows to a maximum of 23 W with a slope of 51% as the launched 976-nm power increases to its maximum value of 49 W (90 W of total coupled pump power). At the same time, the Stokes waves at the 1st and 2nd order Stokes peaks of the 950-nm pump disappear. The reason is that the pumping of the 1st Stokes peak at ~990 nm decreases as the depletion rate of the 950-nm pump increases due to increasing SRS into 976 nm. Although the radiation at 976 nm and 1020 nm adds to the Raman gain at 1045 nm, this is apparently not enough to compensate the reduction in Raman gain from the 990-nm wave. We expect the 1045-nm Stokes would reappear at higher pump power, but can then be suppressed with a shorter fiber or intra-cavity filtering.

Lastly, we set the 976-nm pump to its maximum power (49 W) and gradually increased the 950-nm pump. The curve (iii) in Fig. 2 shows the output power and Fig. 3(c) shows the spectra at different pump powers. The inset of Fig. 2 shows a typical 2D power distribution, at maximum pump as reconstructed by a beam profiler (Thorlabs BP104-IR) from the 1D distributions it measured in orthogonal transverse directions. As we did that, the wavelength of the 950-nm pump increased from 946 nm to 956 nm because of the heat. The output power increased from 7.8 W to 21.3 W when we added 41 W of the 950-nm pump for a slope efficiency of 31%. This slope efficiency is comparable to the 36% achieved with 976-nm single-diode pumping. The slight reduction from 23 W may be caused by a degraded alignment. The beam quality factors (M^2) averaged for the two orthogonal axes were measured to 4.1, 4.6, and 5.2 for 7.8 W, 14.1 W, and 21.3 W of output power, respectively, for a

TABLE I
BRIGHTNESS ENHANCEMENT

Launched pump power, 976 nm + 950 nm [W]	Brightness of signal (B_s) [W·sr^{-1}·μm^{-2}]	BRIGHTNESS OF PUMP (B_p) 976 nm + 950 nm [W·sr^{-1}·μm^{-2}]	Brightness Enhancement (B_s / B_p)
49.1 + 0	0.46	0.16 + 0.00	2.8
49.1 + 18.4	0.64	0.16 + 0.06	2.9
49.1 + 41.4	0.76	0.16 + 0.14	2.5

brightness of 0.76 W·sr^{-1}·μm^{-2} at maximum power. The beam quality factors of the launched pump within the GRIN fiber is around 18 with the assumption that all the modes are equally excited. From this, the full-power brightnesses of pumps in the fiber are calculated to 0.16 W·sr^{-1}·μm^{-2} (976 nm) and 0.14 W·sr^{-1}·μm^{-2} (950 nm). This shows that the enhancement of brightness for the maximum output power (21.3 W) is a factor of ~2.5 from the brightness of the combined pumps, and a factor of ~4.76 from the 976-nm pump alone. Table 1 summarizes the brightness enhancement.

IV. SIMULATIONS

In our previous work [6] with spectrally narrow pumping of a longer piece (1.5 km) of the same fiber, we reached a significantly higher slope efficiency (80%) than now (51%). Although the difference in fiber length and propagation loss may explain some of this, the much wider pump spectrum we have now will also reduce the efficiency, as shown in the experiments. We investigated this further with simulations. We considered a simplified system with three bi-directional waves at 950 nm, 976 nm, and 1020 nm (i.e., the two pumps and the primary Stokes wavelength), according to the following coupled differential equations:

$$\pm\frac{1}{P_i^{\pm}}\frac{dP_i^{\pm}}{dz} = -\alpha_i + \left(\sum_{i>j}\frac{g_{R_{ij}}}{A_{i,j}}\left(P_j^{+}+P_j^{-}\right) - \sum_{i<j}\frac{g_{R_{ij}}}{A_{i,j}}\left(\frac{\lambda_j}{\lambda_i}\right)\left(P_j^{+}+P_j^{-}\right)\right),$$

$$with\ i,j = 1,2,3$$

These equations are a straightforward extension of common Raman equations [1] to multi-wavelength bi-directional propagation. The wavelengths λ_1, λ_2, and λ_3 correspond to 950 nm, 976 nm, and 1020 nm, respectively, and α_i is the background loss and $P_i^{\pm}$ is the power in channel (wave) i. The superscript +/– indicates the direction of propagation. Furthermore, $g_{R_{ij}}$ is the Raman gain coefficient between λ_i and λ_j, and $A_{i,j}$ is the effective area for the interaction, which is inversely proportional to the intensity overlap between wave i and j. Note that this model implies that the excited modes in one wave are coupled so that all light propagating in one direction at one wavelength can be treated as a single entity. Otherwise, A_{ij} would change along the fiber. This was a restriction of the simulation software. The near- and far-end cavity reflectances were set to 0.04 and 0.8, respectively, for all waves.

Fig. 4 shows the results of our simulations, together with

This article has been accepted for publication in a future issue of this journal, but has not been fully edited. Content may change prior to final publication. Citation information: DOI 10.1109/LPT.2018.2863559, IEEE Photonics Technology Letters

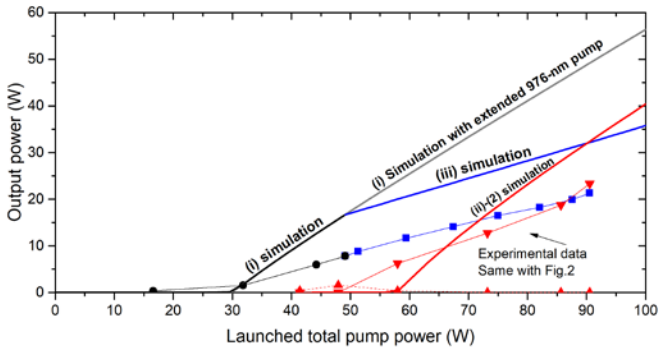

Fig. 4. Simulations, together with experimental data. High-power single wavelength 976-nm pumping (grey line) is also shown. Labeling as in Fig. 2.

experimental data. Here, we assumed that the pump intensity distribution everywhere along the fiber was given by the sum of the intensity distribution of lowest 109 modes with equal power, out of a total of 351 modes. Although we believe more modes than that are actually excited at the launch, this gave good agreement with the experimentally determined threshold. For the signal distribution, we assumed that only the 13 lowest modes were excited, with equal power. This is motivated by the signal measured beam quality, which is significantly better than the value (M^2 = 18) if all signal modes are equally excited. Based on these distributions, we then calculated effective Raman gain coefficients as the local Raman gain coefficient for the wavelengths in question weighted by the intensity distributions of the interacting waves. In turn, the local Raman gain coefficient was determined from the local Ge-concentration, which is proportional to the local increase in the refractive index [11], [12]. The gain coefficients become 6.40 × 10^{-14}, 9.17 × 10^{-15}, and 1.19 × 10^{-13} m/W for $g_{R_{12}}$, $g_{R_{13}}$, and $g_{R_{23}}$, respectively. The effective areas were calculated by estimating the overlap between waves in the same manner as in ref. [13]. They become $A_{1,2}$ = 1559 μm^2 and $A_{1,3} = A_{2,3}$ = 985 μm^2. Likewise, the loss coefficients were determined from the intensity distributions and the dependence of the loss on the wavelength and the (local) Ge-concentration [12], [14]. They become 5.7, 4.8, and 5.2 dB/km for α_1, α_2, and α_3, respectively. These are higher than the experimental values for the 500-m long fiber. Given that the local loss varies between ~ 1 dB/km and 6.5 dB/km depending on the local Ge-concentration, this can perhaps be explained by differences in the intensity distributions.

The agreement with experiments is still relatively poor, and we found it difficult to improve it within our simple model. The reason for this may be that the modes cannot be treated as a single entity and therefore propagate with different loss and Raman gain. It was still possible to achieve good agreement with experiments, if we assume that an increasing number of modes are excited at higher power levels. This has some support from the beam quality values in Table 1, although the quantitative agreement was modest. A model which better describes the spectral evolution and the mode-coupling may be needed to improve the agreement with experiments.

We can still use our simplified model to estimate the penalty of dual-wavelength *vs*. single-wavelength pumping at 976 nm (also shown in Fig. 4). When the 976-nm pump is at full power (49 W), an increase in the 950-nm pump yields a slope efficiency of 37%. The output power reaches 32 W when the 950-nm pump reaches its full 41 W of power. If instead the 976-nm pump is increased beyond 49 W, the slope efficiency becomes 78%. This difference is significant, but we note that the experimental difference in slope is smaller. Furthermore, the brightness of available diode lasers is limited, and launching more power at a single wavelength may not be possible. Note further that also in the simulations, the conversion efficiency is higher with dual-wavelength pumping (32 W / 90 W = 36%) than with single-wavelength pumping (16 W / 49 W = 34%). We also found that realistic reductions in fiber loss reduced the difference between the slope efficiencies for 950-nm and 976-nm pumping.

V. Conclusion

We have demonstrated efficient high-power pumping of a fiber Raman laser with two wavelength-combined multimode diode lasers at 950 and 976 nm. Although the spectral separation of 270 cm^{-1} is both substantially larger than the Raman linewidth of ~ 100 cm^{-1} and substantially smaller than the Raman peak shift of 440 cm^{-1}, the addition of the 950-nm diode almost triples the output power. We believe that our results prove the viability of efficient pumping of fiber Raman lasers with spectrally broad wavelength-combined diode lasers sources currently being developed for materials processing.

References

[1] G. P. Agrawal, *Nonlinear fiber optics*, 4th ed. London: Academic Press, 2006.
[2] V. R. Supradeepa *et al.*, "Raman fiber lasers," *J. Opt.*, vol. 19, no. 2 (art. no. 023001), 2017.
[3] L. Zhang *et al.*, "Kilowatt Ytterbium-Raman fiber laser," *Opt. Express*, vol. 22, no. 15, pp. 18483–18489, 2014.
[4] J. Ji, C. A. Codemard, and J. Nilsson, "Brightness enhancement limits in pulsed cladding-pumped fiber Raman amplifiers," in *Proc. SPIE, Fiber Lasers VII: Technology, Systems, and Applications*, 2010, p. 75801L.
[5] Y. Glick, V. Fromzel, J. Zhang, N. Ter-Gabrielyan, and M. Dubinskii, "High-efficiency, 154 W CW, diode-pumped Raman fiber laser with brightness enhancement," *Appl. Opt.*, vol. 56, no. 3, pp. B97, 2017.
[6] T. Yao, A. Harish, J. Sahu, and J. Nilsson, "High-Power Continuous-Wave Directly-Diode-Pumped Fiber Raman Lasers," *Appl. Sci.*, vol. 5, no. 4, pp. 1323–1336, 2015.
[7] J. Malchus, V. Krause, G. Rehmann, M. Leers, A. Koesters, and D. G. Matthews, "A 40kW fiber-coupled diode laser for material processing and pumping applications," in *Proc. SPIE, High-Power Diode Laser Technology and Applications XIII*, 2015, p. 934803.
[8] A. Sanchez-Rubio *et al.*, "Wavelength Beam Combining for Power and Brightness Scaling of Laser Systems," *Lincoln Lab. J.*, vol. 20, no. 2, pp. 52–66, 2014.
[9] S. Aparanji, V. Balaswamy, S. Arun, and V. R. Supradeepa, "Simultaneous Power Combining and Wavelength Conversion of High Power Fiber Lasers," in *Laser Congress 2017 (ASSL, LAC)*, 2017, paper ATu3A.4.
[10] S. Hong, Y. Feng, and J. Nilsson, "Multi-Wavelength Diode-Pumping of Fiber Raman Laser," in *Conference on Lasers and Electro-Optics*, 2018, paper SM1K.6.
[11] S. T. Davey, D. L. Williams, B. J. Ainslie, W. J. M. Rothwell, and B. Wakefield, "Optical gain spectrum of GeO_2-SiO_2 Raman fibre amplifiers," *IEE Proc. J - Optoelectron.*, vol. 136, no. 6, pp. 301–306, 1989.
[12] J. W. Fleming, "Dispersion in GeO_2–SiO_2 glasses," *Appl. Opt.*, vol. 23, no. 24, pp. 4486–4493, 1984.
[13] K. Rottwitt, J. Bromage, A. J. Stentz, L. Leng, M. E. Lines, and H. Smith, "Scaling of the Raman gain coefficient: Applications to germanosilicate fibers," *J. Light. Technol.*, vol. 21, no. 7, pp. 1652, 2003.
[14] M. N. Zervas and R. I. Laming, "Rayleigh Scattering Effect on the Gain Efficiency and Noise of Erbium-Doped Fiber Amplifiers," *IEEE J. Quantum Electron.*, vol. 31, no. 3, pp. 468–471, 1995.